Research Article

Isotherm and thermodynamic studies of 2,4,6 Tichlorophenol onto newly adsorbents based zeolite as an efficient adsorbents

Atyaf Khalid Hameed[1] · Mohd Hasbi Ab. Rahim[2] · Nugroho Dewayanto[3] · Mohd Ridzuan Nordin[4]

Abstract
The aim of this study is to evaluate the adsorption efficiency of using zero valent iron supported on carbon-coated zeolite NZVI/SuZSM and zeolite NZVI/ZSM and as developed adsorbents for the removal of 2,4,6- Trichlorophenol (TCP) from aqueous solution. The characteristic of the adsorbents was conducted via XRD, BET (SBET), TGA, FTIR, FESEM-EDX, and TEM examination. In addition, the impact of different parameters such as contact time, initial concentration, pH and temperature were studied. The experimental data investigated by Langmuir and Freundlich adsorption isotherms and two models for kinetic studies of pseudo-first-order and pseudo-second-order models. The results indicated that the adsorption studies fitted well with Langmuir for the adsorbent NZVI/SuZSM and fitted well with Freundlich for the adsorbent NZVI/ZSM. In addition, both models fitted the data well but pseudo-second-order models more favorable with correlation values of R2 of 0.9995 and 0.9994 more than first order models for the adsorbents NZVI/ZSM and NZVI/SuZSM, respectively. The equilibrium time was achieved after 90 min for both adsorbents. Depending on the Langmuir model, the maximum adsorption capacities were 22.27 mg/g and 30.58 mg/g for NZVI/ZSM and NZVI/SuZSM, respectively at (27 °C ± 2). The thermodynamic parameters indicated that adsorption of TCP onto NZVI/ZSM was an endothermic and non-spontaneous process in temperature of 30 °C, while the adsorption of TCP onto NZVI/SuZSM was an endothermic and spontaneous process. The synthesize adsorbents (NZVI/ZSM and NZVI/SuZSM) could be applied as an efficient adsorbent for the removal of TCP from aqueous solution.

Keywords Supported nano zero valent iron · 2,4,6-Trichlorophenpl adsorption · Carbon coated materials · Adsorption · Kinetic studies · Thermodynamic aspect

1 Introduction

The development of the chemical industry has produced increasing the disposal of pollutants, especially organic pollutant. Wastewater contains chlorophenol pollutants generated from pharmaceuticals, paper, wood, pesticide, solvent, paint, industries, and water disinfecting process [4]. These persistent organic pollutants (POPs) have existed in water and soil because they have three chloride groups linked to the phenol ring. The 2,4,6-Trichlorophenol (TCP) is one of POPs compound and it is harmful to wildlife and human as well as listed as precedence–controlled pollutant by the United States Environmental Protection Agency (USEPA). The TCP compound was toxic, carcinogenic and mutagenic. Also reiterate and long exposures can cause kidney, Liver, bone and neurological marrow disorders and also the loss of anemia, appetite, and weight loss. Thus, TCP presence in water resources even at low concentrations is injurious to aquatic organisms and human health. According to the chemical characteristics and

✉ Atyaf Khalid Hameed, atyaf.ump2015@gmail.com | [1]Environmental and Water Research Technology Directorate, Ministry of Sciences and Technology, Al-Jadirya, Baghdad, Iraq. [2]Faculty of Industrial Sciences and Technology, University Malaysia Pahang, Lebuhraya Tun Razak, 26300 Kuantan, Pahang, Malaysia. [3]University Kuala Lumpur, Malaysian Institute of Chemical and Bioengineering Technology, Vendor City 1988, 78000 Alor Gajah, Melaka, Malaysia. [4]Faculty of Technology Management and Technopreneurship, University Technical Malaysia Melaka, Hang Tuah Jaya, 76100 Durian Tunggal, Melaka, Malaysia.

SN Applied Sciences (2019) 1:419 | https://doi.org/10.1007/s42452-019-0425-4

Received: 26 February 2019 / Accepted: 27 March 2019 / Published online: 5 April 2019

environmental impacts of TCP and the inefficiency of conventional treatment methods for the complete removal of it from the aquatic solution, applying of advanced, quick and effective techniques, is essential.

Several methods have been investigated for the removal of chlorinated phenols, such as chemical, physical and biological treatment by using dead fungus, catalytic wet oxidation, advanced oxidation process (AOP), photocatalytic process, ion-exchange and adsorption techniques performed by Bandstra et al. [5] and Hameed et al. [15]. Most of these methods were expensive and inefficient. Thus, the adsorption of TCP from aqueous solution onto different types of an adsorbent considered as a superior method. Previously, the adsorption of TCP was limited to it is isotherm and kinetic aspect [19].

Zeolite was microporous, aluminosilicate minerals commonly used as adsorbents for several pollutants [20]. Zeolites, in general, were characterized by high specific surface areas and high cation exchange capacities (CECs). Their rigid three-dimensional structures make it free of the shrink/swell behavior. For these reasons, zeolites can offer superior sorption, hydraulic properties and have found use as molecular sieves and sorbents in wastewater treatment [32].

Activated carbon, due to its structure and high surface area, has been proposed as an adsorbent, and a suitable option for the effective removal of organic contaminations. But using of it in large scales (in engineering processes) has been limited because of problems such as filtration, dispersion, create turbidity and high cost of its reduction [3, 19]. Some developments methods in the forming of carbonaceous layer on mesoporous material taken place in order to overcome the above problems. Carbon coated mesoporous materials may be prepared by inundate the coating of mesoporous structure into a carbon source solution, e.g. furfural alcohol and polymer [13, 24]. In addition to the filling, carbon coating was also a very important process not only to enhance the functionality but also to give new functions to porous inorganic materials, as recently reviewed by De la Torre et al. [8]. Therefore, the resulting carbon-coated materials could be applied for the electro-chemical fields such as a porous electrode for super capacitor, fuel cell and biosensor [16].

To illustrate, if the whole surface including the pore walls, zeolite (ZSM-5) was completely and uniformly coated with carbon layer like a single graphene sheet, the coating could endow the mesoporous materials with both good chemical stability and electrical conductivity [25, 31] with keeping their original excellent features such as uniform mesopores, size-controllable pores and high surface area. When once zeolite surface was saliyated with silanol groups, the surface become very active toward the pyrolytic carbon deposition at as low a temperature as 500 °C and thereby uniform carbon deposition could be easily achieved [33] by a simple carbon coated process using carbon precursor.

To the best of our knowledge, utilization of D-glucose as carbon coating precursor on mesoporous materials does not have been investigated so far. The objectives of the present study was to synthesize and characterize a Nano zero valent iron supported on zeolite (NZVI/ZSM) and Nano zero valent iron supported on carbon-coated zeolite (NZVI/SuZSM) adsorbents, assess its efficiency for TCP removal and studding the isotherm, kinetic and thermodynamic aspect of the prepared adsorbents.

2 Methodology

2.1 Materials

Sodium borohydride ($NaBH_4$) 98.5%, iron (III) chloride hex hydrate ($FeCl_3{\cdot}6H_2O$) 99% were obtained from Merck. 2, 4, 6-Trichlorophenol was supplied by the Aldrich Co. with a purity of 99.8%. ZSM-5 (Si/Al = 30) was supplied by Zeolyst International. D-glucose with purity 99% is purchased from Merck. The 2-propanol (chromatography grade), and KBr (IR spectroscopy grade) were purchased from Merck Millipore. Sodium hydroxide (NaOH) and hydrochloric acid (HCl) were obtained from Sigma-Aldrich, while analytical grade absolute ethanol and acetone were obtained from Merck and used directly without purification. Nitrogen for carbon coating step was also supplied by MOX-Linde. Sodium hydroxide (NaOH) and hydrochloric acid (HCl) were obtained from Sigma-Aldrich.

2.2 Preparation and characterization

Modification of ZSM-5 (Zeolyst International) was conducted by impregnation of 4 g ZSM-5 with 100 mL from D-glucose solution (4 g/L) under stirring for 3 h at room temperature (27 °C ± 2). The mixture was centrifuged and decanted to collect the solid and dried in an oven at110 °C for 12 h. The solid was then carbonized in a furnace at a coveted temperature (500 °C) for 2 h in inert condition obtained by flowing N_2 gas. Preparation of NZVI/ZSM and NZVI/SuZSM was carried out by introducing one gram and of modified carbon coated zeolite into Fe^{3+} solution, prepared by dissolving 0.4 g $FeCl_3{\cdot}6H_2O$ (from Merck) in 25 mL distilled water. Amount of one gram $NaBH_4$ (Merck) dissolved in 50 mL distilled water adding drop wisely (3 mL/min). The samples were filtered, washed via acetone and dried in an oven at 60 °C for 60 min. The prepared adsorbents were characterized using the N_2 physisorption to evaluate the surface area and the porosity at 105 °C prior to the analysis and the adsorption of N_2 was measured at

– 196 °C by Micrometrics ASAP 2020. The thermal gravimetric analysis (TGA) was carried out by Mettler Toledo TGA/DSC equipped with STAR1 software in order to adjust the weight loss as temperature increases. Nitrogen of flow rate of 50 mL/min was used as cell gas, the X-ray analysis (XRD) was conducted via Rigaku instrument, FTIR analysis was carried out by using Perkin Elmer Spectrometer 100, FESEM equipped with EDX (JEOL) and TEM (Tecnai G2 F20).

Modification of ZSM-5 (Zeolyst International) was conducted by impregnation of 4 g ZSM-5 with 100 mL from D-glucose solution (4 g/L) under stirring for 3 h at room temperature (27 °C ± 2). The mixture was centrifuged and decanted to collect the solid and dried in oven at 110 °C for 12 h. The solid was then carbonized in furnace at coveted temperature (500 °C) for 2 h in inert condition obtained by flowing N_2 gas. Preparation of NZVI/ZSM and NZVI/SuZSM was carried out by introducing one gram and of modified carbon coated zeolite into Fe^{3+} solution, prepared by dissolving 0.4 g $FeCl_3{\cdot}6H_2O$ (from Merck) in 25 mL distilled water. Amount of one gram $NaBH_4$ (Merck) dissolved in 50 mL distilled water adding drop wisely (3 mL/min). The samples were filtered, washed via acetone and dried in oven at 60 °C for 60 min. The prepared adsorbents were characterized using the N_2 physisorption to evaluate the surface area and the porosity at 105 °C prior to the analysis and the adsorption of N_2 was measured at – 196 °C by Micrometrics ASAP 2020. The thermal gravimetric analysis (TGA) was carried out by Mettler Toledo TGA/DSC equipped with STAR1 software in order to adjust the weight loss as temperature increases. Nitrogen of flow rate of 50 mL/min was used as cell gas, the X-ray analysis (XRD) was conducted via Rigaku instrument, FTIR analysis was carried out by using Perkin Elmer Spectrometer 100, FESEM equipped with EDX (JEOL) and TEM (Tecnai G2 F20).

2.3 Adsorption study

The adsorptions of the 2-, 4-, 6-Trichlorophenol (TCP) onto the adsorbents are conducted in a batch experiment. The amount of adsorbent was added into the TCP solution (of certain concentration) in the 250 mL conical flasks. The flasks are placed on the orbital shaker operating at 150 rpm in room temperature (27 ± 2 °C). The initial and final concentrations of TCP was determined by using UV spectrometer (Genesys 10S UV–VIS spectrophotometer) at $\lambda_{max} = 310$.

2.4 Isotherm study

The analysis of the pollutant adsorption process could be evaluated by the isotherm studies. The distribution of the molecules between the liquid and the solid phase could be conducted by isotherm studies at the equilibrium rate. However, for the investigation of the sorption isotherm, Langmuir and Freundlich isotherm models are widely used [33].

Monolayer adsorption can be described by the Langmuir isotherm model. The initial of the maximum adsorption capacities corresponds to a saturated homogeneous adsorbent surface with equal energy sites that are equally available for the adsorption and monolayer of solute molecules. The energy of the adsorption process was constant and there is no transmigration of TCP in the plane of the surface [22] Langmuir isotherm model can express as Eq. 1:

$$q_e = q_m b c_e + b c_e \tag{1}$$

where q_e is the adsorbate on the adsorbent (mg/g), q_m is the maximum adsorption capacity of monolayer coverage (mg/g), b is the constant related to the binding site (L/mg), and c_e is the concentration of molecule in the solution at equilibrium (mg/L).Multilayer sorption can be described by the Freundlich model. It is used to analyse the adsorbent capacity in wastewater treatment. The adsorption on a heterogeneous surface is well described by the Freundlich model. In this model, the amount of solute adsorbed onto a given mass of sorbent is not constant at different concentrations [2].The non-linear and linear Freundlich models are expressed in Eqs. 2 and 3, respectively:

$$q_e = k c_e \frac{1}{n} \quad \text{(Non-linear form)} \tag{2}$$

$$\log q_e = \log k + \frac{1}{n} \log c_e \quad \text{(Linear form)} \tag{3}$$

where k, constant value consider as adsorption capacity indicator of the adsorbent (mg/g) in adsorption process. $\frac{1}{n}$ constant for the intensity of the adsorption. The q_e was the adsorbate on the adsorbent (mg/g), and c_e is the concentration at equilibrium (mg/L). Both n and K and are constants, used to indicate the linearity and the non-linearity between the adsorbate solution concentrations and the uptake values in the adsorption process. The $n < 1$ indicates poor adsorption. For $2 < n < 10$, it indicates good adsorption as reported by Gurses et al. [12].

2.5 Kinetic study

The effect of time on the adsorption capacity can be evaluated by kinetic studies. A number of models was tested to identify the mechanism of the adsorption process such pseudo-first-order kinetic model and pseudo-second-order kinetic model. The first order model equation was the common adsorption model for the sorption of the solid/liquid phase [27] the Eq. 4, could be applied as follows:

$$Ln\left(q_e - q_t\right) = Lnq_e - k_1 t \tag{4}$$

where t, is the time, q_e is the adsorbate amount at equilibrium time (mg/g), q_t is the adsorbate amount at time t (mg/g), k_1 is the rate constant of pseudo first order model (1/min).The kinetic for pseudo-second-order model can be described as Eq. 5:

$$dq/dt = k_2\left(q_e - q_t\right)^2 \quad (5)$$

where k_2 is the rate constant of the pseudo second order model, (g mg^{-1} min^{-1}) which can be calculated from the slop of plot t/q_t versus t, q_e was the adsorbate amount at equilibrium time (mg/g), q_t is the TCP amount at time t(mg/g).

2.6 Thermodynamic study

In environmental engineering practice, both energy and entropy factors must be considered in order to determine which process will occur spontaneously [34]. The thermodynamic parameters are calculated for this system by using Eq. 6 [30]:

$$lnk_d = \frac{\Delta S^\circ}{R} - \frac{\Delta H^\circ}{RT} \quad (6)$$

where k_d = distribution coefficient (L/g), ΔH° = enthalpy (kJ/mol), ΔS° = entropy (J/mol K), T = temperature (K) and R = gas constant (8.314 J/mole K).

3 Result and discussion

3.1 Characterization

3.1.1 TGA analysis

Figure 1a shows the weight loss of ZSM within 90–110 °C. It occurs due to the loss of the hydrate surface water and the condensations of the alumina groups (Al–OH) and the

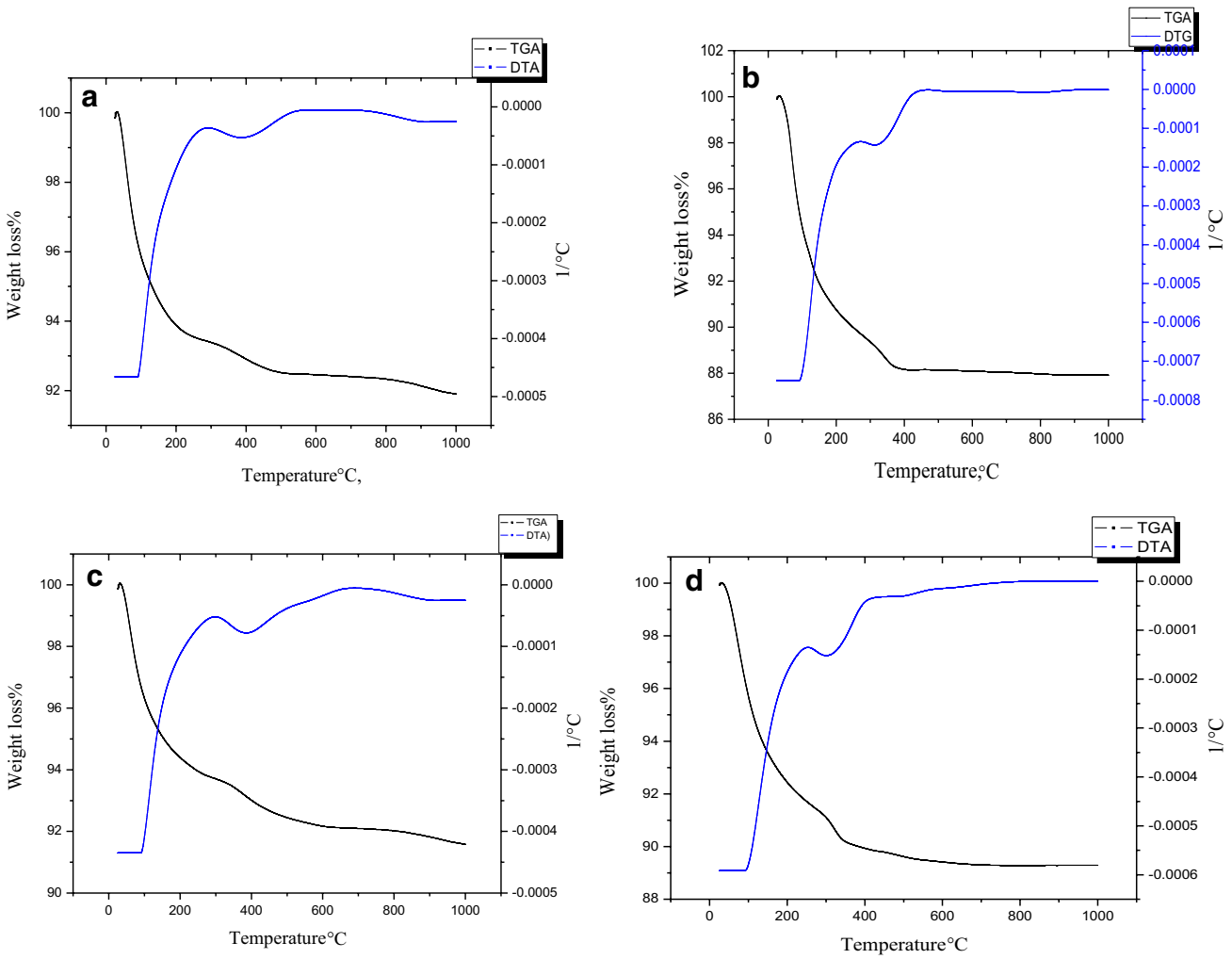

Fig. 1 TGA and DTA for **a** ZSM, **b** NZVI/ZSM, **c** SuZSM and **d** NZVI/SuZSM

silanol groups (Si–OH) to Al–O–Al and Si–O-Si, respectively. The weight loss occurred within 365–600 °C was due to the decomposition of the ZSM. Figure 1b shows the weight loss of NZVI/ZSM within 100–240 °C. It occurs due to the loss of hydrate surface water and residual ethanol. Also, Fe–OH was transformed into FeO or Fe^0. Within 300–500 °C, the weight loss is due to the decomposition of the Fe–O–Al and Fe–O–Si bonds of the adsorbent NZVI/ZSM. Above 500 °C, no significant weight loss is observed. From Fig. 1c, the weight loss pattern of SuZSM is somewhat different from that of ZSM due to the grafting with D-glucose. Within 90–320 °C, weight lose occurs due to the loose of residual water and ethanol. At temperature ranging from 530 to 600 °C, decomposition of the adsorbent SuZSM occurs. Above 600 °C, no significant weight loss is observed. Figure 1d shows the weight loss of NZVI/SuZSM within 100–240 °C which is mainly due to the loss of residual water. Within 390–480 °C, decomposition of adsorbent occurs. Above 500 °C, no significant weight loss appears. The results above show that the stability enhancement of SuZSM was more pronounced than that of ZSM when carbonization via D-glucose is performed.

3.1.2 XRD analysis

The XRD diffractions of NZVI/ZSM and NZVI/SuZSM are illustrated in Fig. 2. The presence of Zero Valent Iron is indicated by a distinct peak at 2θ of 44.45° with detection (1 1 1), which is related to *α*-Fe (NZVI) as observed in the diffractogram of NZVI/ZSM. It appears that the ZeroValent Iron is successfully loaded into the substrate. As illustrated in Fig. 4, the peaks are observed at 2θ of 8.22°, 9.09°, 23.36°, 24.15°, 24.61° and 30.12° which are related to the crystalline structure of ZSM-5 [6]. The presence of carbon-coated surface on NZVI/SuZSM is indicated by the graphite phase at 2θ of 26.92°, 31.56°. On the other hand, the peak observed at 2θ of 34.50° is related to the ZSM-graphite. The apparent peak at 2θ of 45.47° is related to the ZSM-graphite-*α*-Fe. These results indicate NZVI is grafted with the carbon layer.

3.1.3 N_2-physisorption analysis

Parameters such as surface area (S_{BET}), pore volume and pore size of adsorbents were summarized in Table 1. The surface areas of NZVI was found to be 40.65 m^2/g. Meanwhile, their pore sizes was 152.70 Å. It was clear that the surface area and the pore size of NZVI obtained by this study was larger than that reported by Ling et al. [23], which may be attributed to different experimental conditions. In addition the surface area of the ZSM-5, carbon coated ZSM-5 (SuZSM) and the prepared adsorbents presented in Table 1.

3.1.4 FTIR analysis

The FTIR spectra of NZVI/ZSM and NZVI/SuZSM are shown in Fig. 3. The broad spectrum of adsorption bands at wavenumbers of 3800 cm^{-1} and 3400 cm^{-1} were related to the intermolecular OH (Si–OH–Si and Al–OH–Al). Also, they are related to H–O–H stretching [7]. The band at wave numbers of 1648 cm^{-1} and 1661 cm^{-1} can be attributed to O–H bending [20]. A combination band of OCH and COH deformations from sugar molecules is indicated by a peak at the wave number of 1408 cm^{-1} in the NZVI/SuZSM spectrum.

Table 1 The surface area (S_{BET}), pore volume and pore size of the prepared adsorbents

Adsorbent	BET (m^2/g)	BJH adsorption pore volume (cm^3/g)	BJH adsorption pore size (Å)
NZVI	40.65	0.165	152.70
ZSM	254.33	0.095	63.28
SuZSM	246.48	0.099	75.96
NZVI/ZSM	116.52	0.055	91.22
NZVI/SuZSM	182.65	0.112	85.40

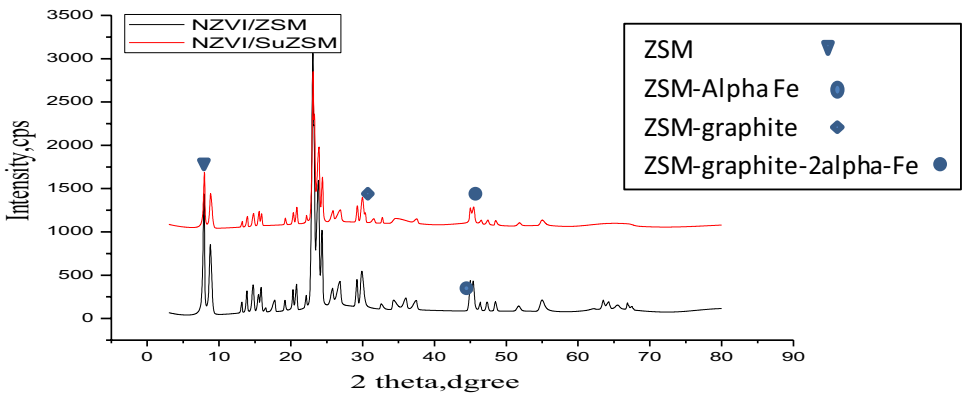

Fig. 2 The XRD diffracton patterns of NZVI/ZSM and NZVI/SuZSM

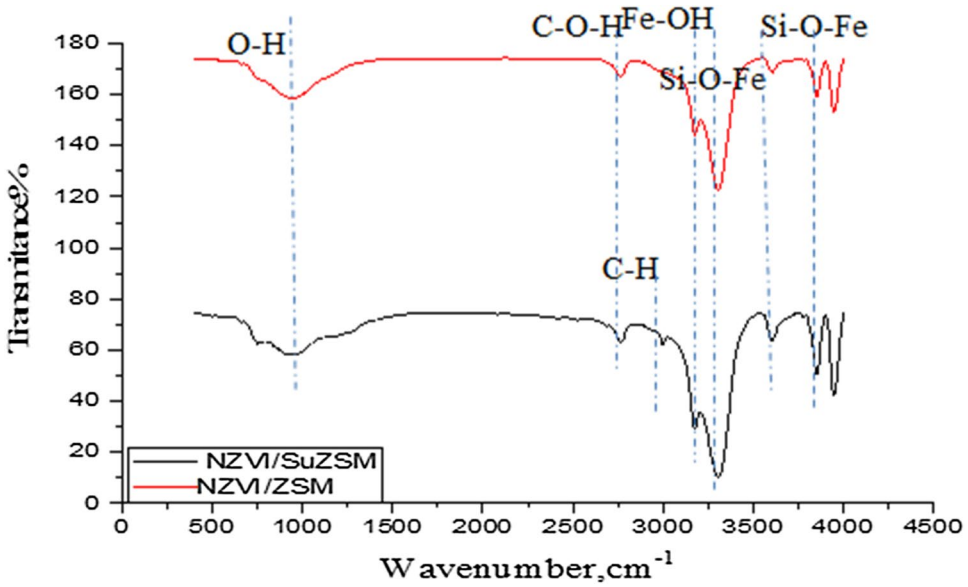

Fig. 3 The FTIR spectra of NZVI/ZSM and NZVI/SuZSM

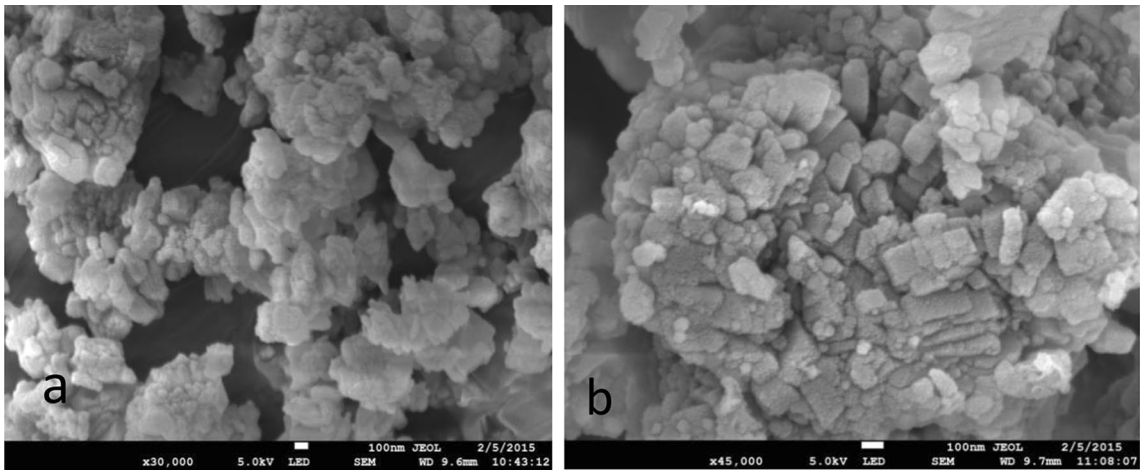

Fig. 4 The FESEM micrograph of **a** NZVI/ZSM at ×30,000 magnification and **b** NZVI/SuZSM at ×45,000 magnification

The absorption band at the wave number of 1237 cm^{-1} in both spectra corresponds to the C–H in-plane bending vibrations [29]. Adsorption bands in both spectra at the wave number of 1114 cm^{-1} are caused by the primary oxygen single bond (–C–O–H) [17], while the bands at wave numbers of 814 cm^{-1} and 819 cm^{-1} were attributed to the formation of SiO–Fe bonds [28]. Moreover, the crystalline structure of ZSM-5 was indicated by vibration peak at around 560 cm^{-1} as observed by Abrishamkar and Izadi [1].

3.1.5 FESEM analysis

The FESEM micrographs of the prepared adsorbents are presented in Fig. 4a, b, showing the morphologies of NZVI/ZSM and NZVI/SuZSM, respectively. It could be b seen that the modification of ZSM-5 by using impregnation of carbon affects the morphology of the substrate due to the change of the particle shape. As seen from Fig. 4a, the surface morphology of NZVI/ZSM was irregular. On the other hand, the surface morphology of NZVI/SuZSM exhibits more regular cubic shapes as shown in Fig. 4b. Furthermore, Fig. 4a, b shows that the iron nanoparticles were dispersed evenly on the surface and the pore of the substrate. This result agrees with the previous observation whereby the surface area of adsorbent was reduced after impregnation with NZVI. However, the surface area of NZVI on the surface of SuZSM was higher than that on the surface of ZSM.

On the other hand, Table 2 shows the weights and the atomic weights for the elements in ZSM-5 surface, i.e. silicon, and oxygen. The atomic/weight values of Si, O,

Table 2 The EDX analysis of ZSM, SuZSM, NZVI/ZSM and NZVI/SuZSM

Adsorbents	Element (%)	Weight (%)	Atomic weight (%)
ZSM-5	O	60.86	73.15
	Si	37.21	25.47
	Al	1.93	1.38
SuZSM	C	14.89	21.12
	O	59.31	63.18
	Al	1.37	0.86
	Si	24.44	14.83
NZVI/ZSM	O	75.63	85.69
	Si	18.55	11.97
	Al	1.29	0.87
	Fe	4.53	1.47
NZVI/SuZSM	O	60.59	69.95
	Si	24.60	16.18
	Al	1.62	1.11
	Fe	6.23	2.06
	C	6.96	10.71

and Al were found to be 25.47%/37.20%, 73.15%/60.86% and 1.37%/1.93%, respectively.

3.1.6 TEM examination

The morphology and the surface distribution of the novel adsorbent were presented in Fig. 5. The cubic structure of ZSM-5 could be seen from the TEM micrograph (black spots) as shown in Fig. 5a. As shown in Fig. 5b, the center black spot was NZVI and the dark layer was carbon coating. Seemingly, the NZVI was surrounded by the carbon layer. As shown in Fig. 5c, the distribution of NZVI on the surface of ZSM was quite even, thereby increasing the reactivity of the prepared adsorbent. Figure 5d shows the bulk structure of the adsorbent which was related to the graphite layer. It seems that there was no obvious chain structure of NZVI on the surface. Figure 5e shows the spherical particles of NZVI on the surface of the adsorbent. The NZVI particle was surrounded by the carbon layer. Finally, Fig. 5f shows that the spherical particles are surrounded by the carbon layer.

3.2 Adsorption parameters

A stock solution of concentration 1000 mg/L of TCP was prepared by dissolving the required amount of adsorbate in 2-Propanol for the preparation of TCP stock solution. The effect of contact time (2–180 min), temperature (30–50 °C), pH (2–9) and initial concentration (10–40 mg/L) were studied. The adsorption properties of NZVI/ZSM and NZVI/SuZSM were evaluated by sorption of TCP. A stock solution of TCP was prepared via dissolving TCP in alcohol as 2-propanol instead of distilled water. The TCP considered stable compound because the resonance of the aromatic structure in addition to the low solubility in water, Cs ofChlorophenol is 210.8 mol/dm^3 as suggested by Kirsanov and Shishkin [21] in addition to the higher acidic strength of chlorine atom.

3.2.1 Contact time

Equilibrium time of adsorption was determined by using 0.1 g of adsorbents (NZVI/ZSM) and (NZVI/SuZSM) in 100 mL of 20 mg/L TCP solutions. The mixture was equilibrated by shaking thoroughly at 150 rpm in orbital shaker. Samples are taken out at different time intervals viz. 2, 4, 8, 15, 30, 60, 90, 120 and 180 min at pH value of 7, in room temperature (27 ± 2 °C). At the end of the shaking period, the solution was sampled by a syringe. The samples were then centrifuged and the supplements are kept for further analysis. The equilibrium time was an important factor to set the adsorption time for each adsorbent and was found to be 90 min for the both tested adsorbents.

3.2.2 Initial concentration

The effect of initial concentration of the TCP on the adsorption performance was carried out through a series of adsorption experiments with different initial TCP concentrations ranging from 10 to 40 mg/L. The experiments were performed by using a 100 mL TCP solution. The adsorbent dosage is 0.1 g/L. The samples used to determine the adsorption performance were available after the batch mixture was stirred for a suitable equilibrium time (90 min) for both adsorbents.

3.2.3 Temperature

To study the temperature effect, the experiment was operating and the thermodynamic parameters such as ΔG°, ΔH°, and ΔS° were then determined. The effects of temperature on the adsorption equilibrium of TCP onto NZVI/ZSM and NZVI/SuZSM were investigated and the results were presented in Fig. 6. Adsorption of TCP increased as temperature increased, indicating the endothermic adsorption process. It was found that the uptake values of NZVI/SuZSM were 16.33 mg/g while the uptake of NZVI/ZSM was 11.93 mg/g.

3.2.4 pH

Different pH values were considered: 2, 4, 7 and 9. The pH of the solution was measured by the pH meter. The

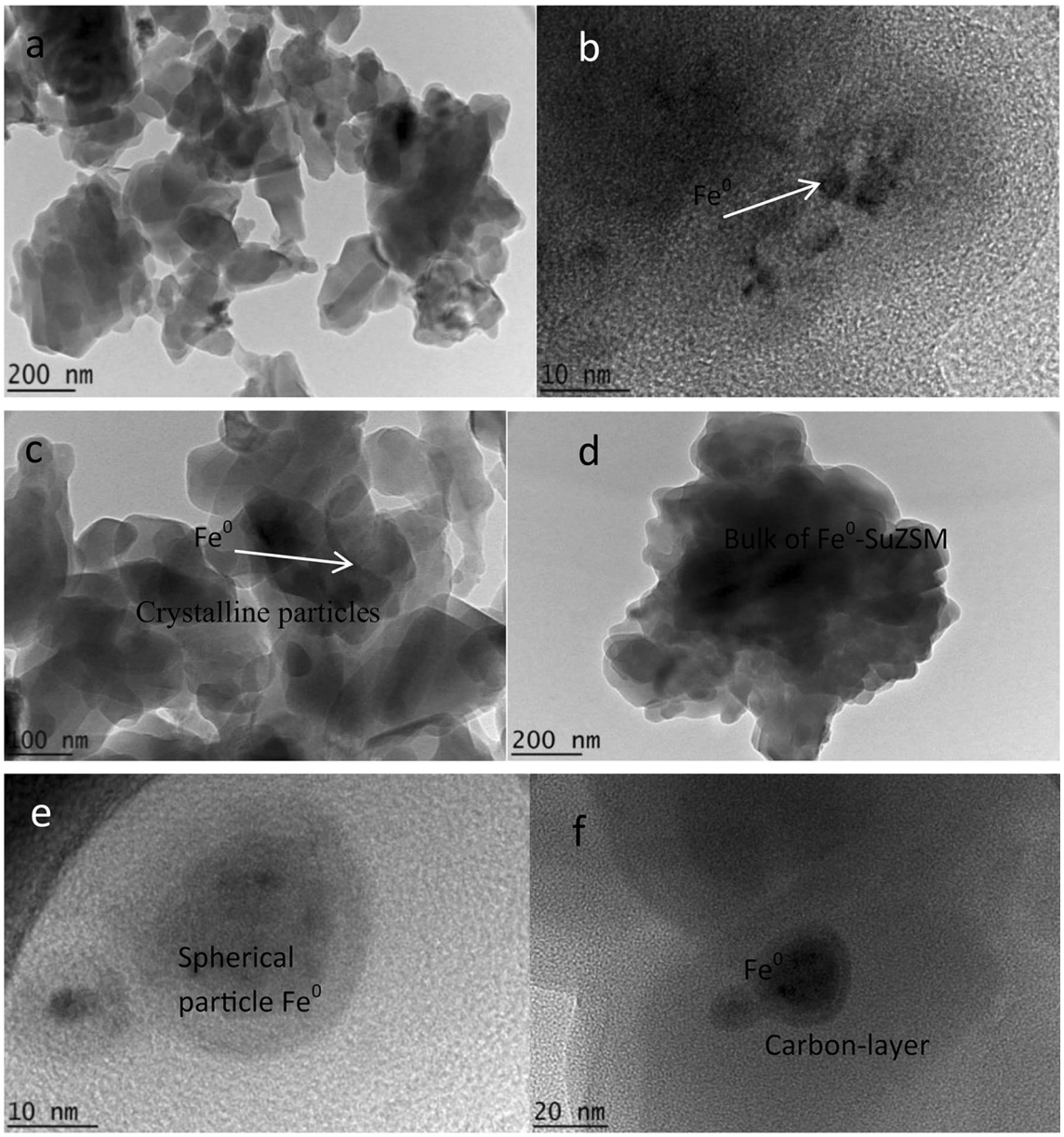

Fig. 5 The TEM examination of NZVI/SuZSM, **a** the crystalline particals of SuZSM surface at 200 nm, **b** the black spots for NZVI surrounded with dark layer of carbon coated at 10 nm, **c** the NZVI loaded on the surface of ZSM and the carbon layer at 100 nm, **d** the bulk structure of the adsorbent at 200 nm, **e** the spherical particle of NZVI at 10 nm and **f** the carbon layer and the dark spots of NZVI at 20 nm

pH-meter was calibrated by using a pH buffer of 4.0, 7.0, and 10 to ensure the accuracy of the pH measurement. The initial pH of the solution was adjusted by using 1 M HCl or 1 M NaOH. Then, the adsorption performance was performed. The effects of pH on the adsorptions of TCP onto NZVI/ZSM and NZVI/SuZSM were illustrated in Fig. 7. The unionized species of halogenated organic compounds were high, which do not favor any repulsion between the adsorbent surface and the molecular species of TCP. Therefore, the electrostatic attractions between the TCP molecules and the adsorption sites increased. Besides, there was competition between the OH^- ions in the adsorbent surface and the ionic species of TCP, hence reducing the TCP removal. The removal values for the adsorbents NZVI/SuZSM and NZVI/ZSM were found to be 83.40% and 62.78%, respectively.

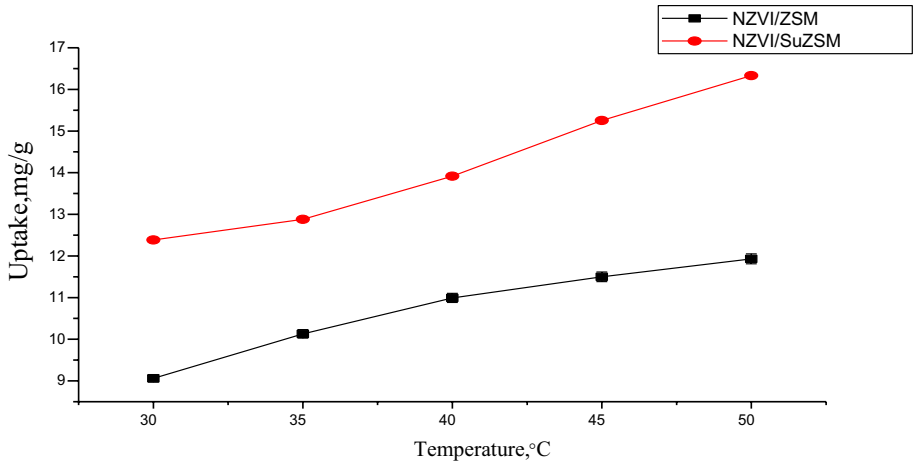

Fig. 6 Effect of adsorption temperature on TCP adsorption onto NZVI/ZSM and NZVI/SuZSM uptake

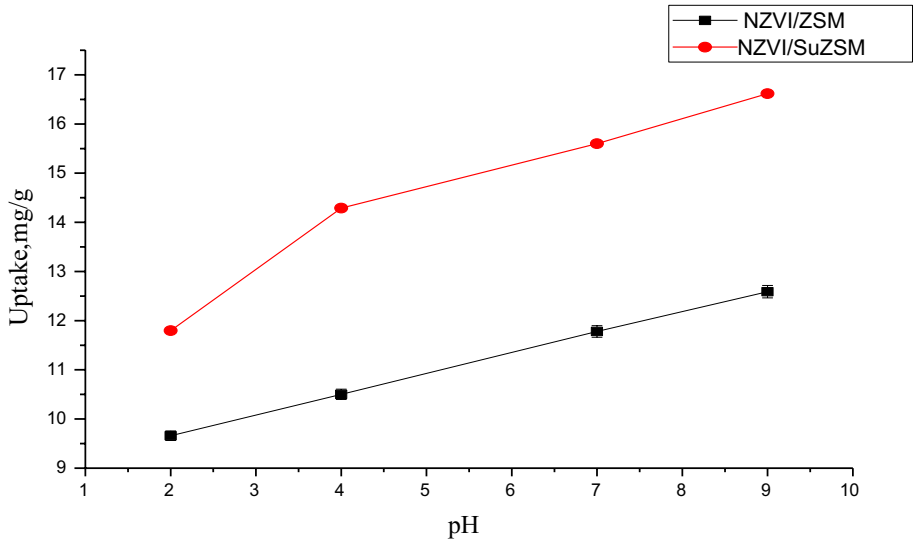

Fig. 7 Effect of initial pH of TCP solution onto NZVI/ZSM and NZVI/SuZSM uptake

3.3 Adsorption isotherm

The isotherm studies are conducted by a series of batch adsorptions. The initial pollutant concentration is ranging from 10 to 40 mg/L.The Langmuir and Freundlich isotherm models for adsorption of TCP onto NZVI/ZSM and NZVI/SuZSM are presented in Fig. 8a, b respectively. The vertical error bars on the data points indicated the average deviation from triplicate the data collection.The Langmuir and Freundlich constants of adsorption of TCP onto NZVI/ZSM are 0.033 L/mg and 1.21 g/L, respectively, while the Langmuir and Freundlich constants of adsorption of TCP onto NZVI/SuZSM are 0.05 L/mg and 2.16 g/L, respectively. The maximum adsorption capacities of TCP onto NZVI/ZSM and NZVI/SuZSM are 22.27 mg/g and 30.58 mg/g, respectively (from Langmuir isotherm). In general, the Freundlich isotherm characterizes the adsorption process better than the Langmuir isotherm for NZVI/ZSM, while Langmuir isotherm characterizes the adsorption process better than the Freundlich isotherm for NZVI/SuZSM. The 1/n value of the Freundlich isotherm is ~ 1.0 for both NZVI/ZSM and NZVI/SuZSM. Hence, the adsorption of TCP onto NZVI/ZSM can be considered as multilayer adsorption while the adsorption of TCP onto NZVI/SuZSM can be considered as monolayer adsorption. The parameters obtained by fitting the results to the Langmuir and Freundlich isotherm models are summarized in Table 3.

From the experimental data, it seems that the fitting errors of both Langmuir and Freundlich isotherm models for NZVI/ZSM and NZVI/SuZSM were smaller than one ($R^2 \sim 1$). However, the Langmuir isotherm model gives a smaller fitting error for the adsorbent NZVI/ZSM than the Freundlich isotherm model indicating multilayer adsorption. On the other hand, the correlation coefficients (R^2) of Langmuir for the adsorbent NZVI/SuZSM of a high value indicating monolayer adsorption. The correlation coefficients (R^2) indicating that the experimental data of the adsorptions for adsorbents as NZVI/ZSM and NZVI/SuZSM

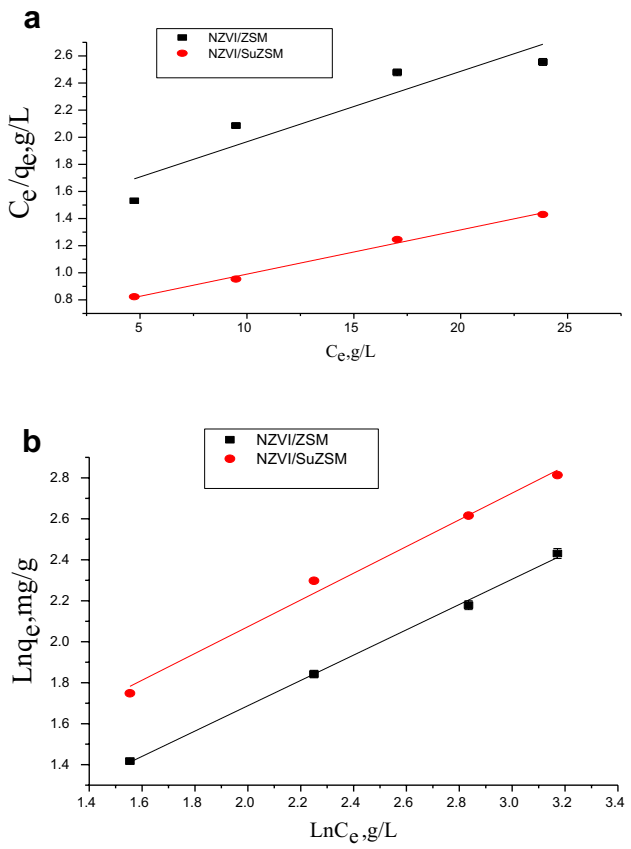

Fig. 8 Adsorption isotherm models of TCP onto NZVI/ZSM and NZVI/SuZSM, **a** Langmuir and **b** for Freundlich models

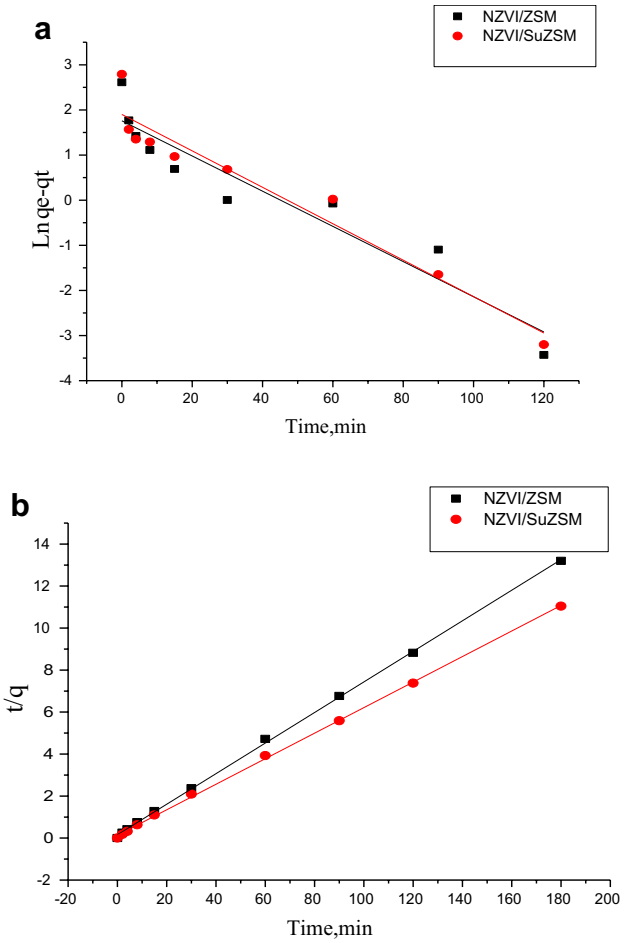

Fig. 9 Linear plot of **a** pseudo-first kinetic model and **b** pseudo-second kinetic model of adsorption of TCP onto NZVI/ZSM and NZVI/SuZSM uptake

are well fitted with both isotherm models. The fitting of the Langmuir and Freundlich isotherm models are summarized in Table 3. Also, the maximum uptake values of all the adsorbents are comparable with other adsorbents reported in Table 3 in monolayer adsorption.

3.4 Kinetic studies

The kinetic studies are conducted by a series of batch adsorptions running at initial pollutant concentration of 20 mg/L. The procedures of kinetic adsorption tests are identical to those of batch equilibration tests. However, the aqueous samples are taken at various time intervals. The result of the kinetic study of TCP adsorption on NZVI/ZSM and NZVI/SuZSM was presented in Fig. 9a, b. It seems that the second order model fits well with the experimental data with a higher R2 value. Thus, it shows that the pseudo-second-order model is more suitable

Table 3 Isotherm parameters of the adsorption of TCP onto NZVI/ZSM and NZVI/SuZSM comparison with literature studies in uptake values

Absorbents	Langmuir			Freundlich			References
	K_L (L/mg)	q_{max}, (mg/g)	R^2	K_f (g/L)	1/N	R^2	
NZVI/ZSM	0.033	22.27	0.9083	1.21	0.65	0.9933	This study
NZVI/SuZSM	0.05	30.58	0.9946	2.16	0.65	0.9915	This study
Activated carbon/loosestrife	0.15	367.64	0.5222	24.06	0.79	0.9009	Fan et al. [9]
surfactant-modified zeolitic tuff	0.023	12.90	0.9901				Naddfi et al. [26]
Activated carbon SKD515	0.40	12.20	0.7800	4.98	0.32	0.9213	Shishkin and Kirsanov [21]
Activated clay	0.022	123.46	0.9300	4.42	0.69	0.9600	Hameed et al. [14]

Table 4 Kinetic parameters of the adsorption of TCP onto, NZVI/ZSM and NZVI/SuZSM were collected in this study

Adsorbents	K_1 (min^{-1})	$q_{e,cal}$ (mg/g)	R^2	k_2 (g/mg min)	$q_{e,cal}$ (mg/g)	R^2	q_e (mg/g)
NZVI/ZSM	0.039	5.81	0.9064	0.034	13.73	0.9995	13.63
NZVI/SuZSM	0.040	6.69	0.9408	0.029	16.29	0.9994	16.29

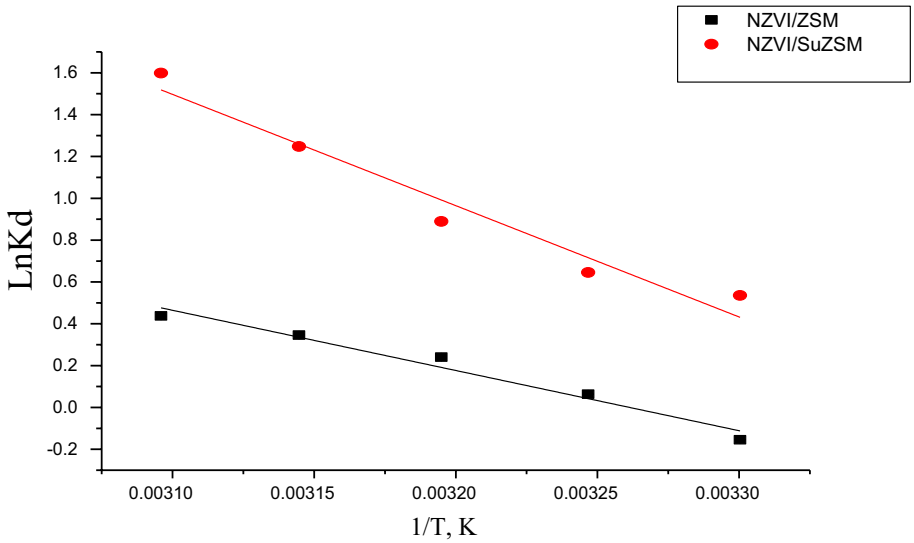

Fig. 10 Van't Hoff plot of effect of temperature on adsorption properties of TCP onto NZVI/ZSM and NZVI/SuZSM

to be applied in the kinetic studies for NZVI/ZSM, and NZVI/SuZSM. The kinetic parameters for the adsorbents such as NZVI/ZSM, and NZVI/SuZSM were summarized in Table 4.

Thus, the experimental data indicates that the pseudo-second-order model is more suitable to be applied in the kinetic studies for NZVI/ZSM, and NZVI/SuZSM and the $q_{e,\ Cal}$ value near to the q_e experimental. The kinetic parameters for the adsorbents NZVI/ZSM and NZVI/SuZSM are summarized in Table 4.

3.5 Thermodynamic studies

Thermodynamic study of adsorption is carried out by equilibrating the TCP solution with an adsorbent at various temperatures ranging from 30 to 50 °C. The thermodynamic studies are conducted by a series of batch adsorptions running at initial pollutant concentration of 20 mg/L. The objectives of this study are to evaluate the changes in enthalpy (ΔH°), entropy (ΔS°) and Gibb's free energy ΔG°) of adsorption [11].

The values of ΔH°, ΔS°, ΔG° are calculated from Fig. 10 and listed in Table 5. Positive ΔH° value indicates endothermic adsorption. This is supported by the fact that the adsorption of TCP increases as temperature increases. The positive ΔS° reveals that the degree of freedom increases at the solid–liquid interface during adsorption. The ΔG° is negative when adsorption happens on NZVI/SuZSM, reflecting the spontaneity of the process. On the other hand, the adsorption process for NZVI/ZSM is un-spontaneous and difficult to apply in practice in temperature 30 °C and thermodynamically feasible in another temperature.

4 Conclusion

In this study, adsorbents such as NZVI/ZSM and NZVI/SuZSM have been successfully synthesized. The prepared adsorbents are characterized by XRD, FTIR, N_2-Physisorption, TGA, TEM, and FESEM-EDX. The performances of NZVI are compared in terms of TCP adsorption with the uptake onto ZSM and SuZSM, and adsorbents such as SuZSM show good performance. For the application of D-glucose as a novel additive in the carbon-coating technique, it is found that the optimal activation temperature is 500 °C. In addition, the carbonization performed via D-glucose increases the adsorption capacity of TCP onto the activated inorganic supports such as ZSM. The modification performed with D-glucose via the wet impregnation method followed by the carbonization step can significantly improve the adsorption rate and the adsorption capacity. The spontaneity of the adsorption process is determined from the free energy ΔG°. Meanwhile, ΔH° indicates the process of whether it is endothermic or exothermic. ΔS° signifies the randomness of the system. Carbon-coated technique leads to improving the physical property of the prepared adsorbents. In addition carbon-coated

Table 5 Thermodynamic parameters for adsorption of TCP onto NZVI/ZSM and NZVI/SuZSM compared with literature review

Adsorbent	ΔH° (kJ/mol)	ΔS° (J/mol K)	ΔG° (J/mol)			References
			303 K	313 K	323 K	
NZVI/ZSM	23.936	78.066	282.038	−498.621	−1279.28	This study
NZVI/SuZSM	44.239	149.59	−1084.63	−2580.48	−4076.33	This study
Montmorillonite	−28.788	81	−3392	−2580	−1769	Fil et al. [10]
MGC-4	87.200	47.22	−20850	−5591.73	6054.6	Wang et al. [33]
Modified malted sorghum mash	38.31	68.16		−21260	−2200	Oyelude and Appiah-Takyi [27]
Mesoporous silica	55.13	235.8		−17654	−19651	Kareem et al. [18]

adsorbents provided higher adsorption efficiency due to the synergistic effect, the available active adsorption site of the supporting materials and the stability of the NZVI. The evaluation of the adsorption performance of the prepared adsorbents was proven via the isotherm studies by Langmuir and Freundlich models. In the kinetic study, the pseudo first order and the pseudo-second-order kinetic models are examined. It seems that the pseudo-second-order kinetic model fits well with the experimental data for both adsorbents. As result the both adsorbents are spontaneity and thermodynamically feasible. This study offers solutions to overcome the industrial wastewater problems especially in the field of organic pollutant removal.

Acknowledgements The author would like to thanks the ministry of science and technology—Iraq for their Scientific supports.

Compliance with ethical standards

Conflict of interest The authors declare that they have no conflict of interest.

Ethical approval This article does not contain any studies with human participants or animals performed by any of the authors.

References

1. Abrishamkar M, Izadi A (2013) Nano-ZSM-5 zeolite: synthesis and application to electrocatalytic oxidation of ethanol. J Microporous Mesoporous Mater 180:56–60
2. Abdel Ghafar HH, Fouad OA, Ali GAM, Makhlouf SA (2013) Enhancement of adsorption efficiency of methylene blue on Co_3O_4/SiO_2 nano composite. J Desalin Water Treat 53(11):2980–2989
3. Atkinson JD, Fortunato ME, Dastgheib SA, Rostam-Abadi M, Rood MJ, Suslick KS (2014) Synthesis and characterization of iron-impregnated porous carbon spheres prepared by ultrasonic spray pyrolysis. J Carbon 49:587–598
4. Aifiei Y, Haoran L, Yali F, Zhuwei D (2015) Mechanism of 2, 4, 6-Trichlorophenol degradation in microbial fuel cells system with microbe isolated from submarine sediment. Int J Electrochem Sci 10:1459–1468
5. Bandstra JZ, Tratnyek PG, Johnson RL, Miehr R (2005) Reduction of 2, 4, 6-Trinitrotoluene by iron metal: kinetic controls on product distributions in batch experiments. J Sci Technol 39:230–238
6. Canli M, Bayca SU, Abali Y (2013) Removal of methylene blue by natural and Ca and K-exchanged zeolite treated with hydrogen peroxide. J Physicochem Probl Miner Process 49(2):481–496
7. Cho YI, Kim BH, Kim SJ, Yun JJ, Lee H, Park SH, Jung SC (2013) Preparation and characterization of zero valent iron powders via transfer type redactor using iron oxide from the acid regeneration process. Adv Powder Technol 24:858–886
8. De la Torre AIR, Dominguez JM, Sandoval G, Torres Rodriguez M, Ramos CE, Melo-Banda JA, Angeles RC (2010) Synthesis of hybrid (Ni-Mo) carbides/carbon-coated mesoporous materials and their catalytic properties for hydrocracking of intermediate paraffins (n-C8). J Catal Today 148(1–2):55–62
9. Fan J, Shi Q, Zhang J, Zhang Ch, Ren L (2011) Adsorption of 2, 4, 6-Trichlorophenol from aqueous solution onto activated carbon derived from loosestrife. J Desalin 267:139–146
10. Fil BA, Korkmaz M, Özmetin C (2012) Cationic dye (methylene blue) removal from aqueous solution by montmorillonite. J Bull Korean Chem Soc 33(10):3184–3190
11. Fungaro D, Borrelyb SI, Izidoro JC, Grosche LC, Pinheiro AS (2010) Adsorption of methylene blue from aqueous solution on zeolite material and the improvement as toxicity removal to living organisms. Orbital- Electron J Chem 2(3):235–247
12. Gurses A, Yalcin M, Bayrak R, Dogar C, Karaca S, Acikyildiz M (2006) The adsorption kinetics of the cationic dye, methylene blue, onto clay. J Hazard Mater 131:217–228
13. Gupta VK, Saleh TA, Agarwal Sh (2011) Synthesis and characterization of alumina-coated carbon nanotubes and their application for lead removal. J Hazard Mater 185(1):17–23
14. Hameed BH, Latiff KN, Ahmad L (2007) Adsorption of basic dye (methylene blue) onto activated carbon prepared from rattan sawdust. J Dyes Pigments 75(1):143–149
15. Hameed BH (2009) Removal of cationic dye from aqueous solution using jackfruit peel as non-conventional low-cost adsorbent. J Hazard Mater 162:344–350
16. Hoshikawa Y, Kyotani T, Komiyam H, Castro-Muniz A, Nanbu H, Yokoyam T, Ishli T (2014) Remarkable enhancement of pyrolytic carbon deposition on ordered mesoporous silicas by their trimethylsilylation. J Carbon 67:156–167
17. Hussein S, Choong Y, Khan MA, Malekbala MR, Thomas S, Cheah W (2011) Carbon coated monolith, a mesoporous material for the removal of methyl orange from aqueous phase: adsorption and desorption studies. Chem Eng J 171(3):1124–1131
18. Kareem SH, Jalhoom MG, Ali IH (2014) Synthesis and characterization of organic functionalized mesoporous silica and evaluate

their adsorptive behavior for removal of methylene blue from aqueous solution. Am J Environ Sci 10(1):48–60
19. Krishnaiah D, Sarbatly R, Anisuzzaman SM, Bono A (2013) Adsorption of 2, 4, 6-Trichlorophenol (TCP) onto activated carbon. J King Saud Univ 25(3):251–255
20. Kim SA, Oh BT, Kannan SK, Kim HM, Lee WH, Lee KJ, Shea PJ, Park YJ (2013) Removal of Pb(II) from aqueous solution by a zeolite–nanoscale zero-valent iron composite. Chem Eng J 217:54–60
21. Kirsanov MP, Shishkin VV (2016) Evaluation and improving the efficiency of the use of activated carbon for the extraction of organo chlorine compound in water technology. Foods Raw Mater 4(1):148–153
22. Lata H, Gupta RK, Garg VK (2007) Removal of a basic dye from aqueous solution by adsorption using Partheniumhysterophorus: an agricultural waste. J Dyes Pigments 74:653–658
23. Ling X, Li J, Zhu W, Zho Y, Shen J, Sun X, Han W, Jiangsu LW (2012) Synthesis of nanoscale zero-valent iron/ordered mesoporous carbon for adsorption and synergistic reduction of nitrobenzene. J Chemosphere 87(6):655–660
24. Malekbala MR, Hussein S, Abdullah LCh, Choong ThSY, Khan MA (2015) Adsorption/desorption of cationic dye on surfactant modified mesoporous carbon coated monolith: equilibrium, kinetic and thermodynamic studies. J Ind Eng Chem 21:369–377
25. Nishihara H, Kwon T, Fukura Y, Iwamura S, Hoshikawa Y, Nakayama W (2011) Fabrication of a highly conductive ordered porous electrode by carbon-coating of a continuous mesoporous silica film. J Chem Mater 23(13):3144–3151
26. Naddafi K, Nabizadeh R, Sarkhosh M, Gholami M, Saeedi R, Rastkari N (2016) Adsorption of 2, 4, 6-Tricholophenol from aqueous solutions by a surfactant-modified zeolitic tuff: batch and continuous studies. J Desalin Water Treat 57(13):5789–5799
27. Oyelude EO, Appiah-Takyi F (2012) Removal of methylene blue from aqueous solution using alkali-modified malted sorghum mash. Turk J Eng Environ Sci 36(2):161–169
28. Petala E, Karakassides MA, Dimos K, Zboril R, Douvalis A, Tucek J, Bakas T (2013) Nano scale zero-valent iron supported on mesoporous silica: characterization and reactivity for Cr(VI) removal from aqueous solution. J Hazard Mater 216(2):295–306
29. Qiu X, Xu Z, Lianga B, Fang Z, Gu F (2011) Degradation of decabromodiphenyl ether by nano zero-valent iron immobilized in mesoporous silica microspheres. J Hazard Mater 193:70–81
30. Sarioglu M, Atay U (2006) Removal of methylene blue by using biosolid. Glob NEST J 8(2):113–120
31. Tumsek F, Koyuncui Z, Bodur G, Bayindir Z (2015) Adsorption of 2,4,6-Trichlorophenol on activated carbon. J Turk Chem Soc, Sect A: Chem 2(3):22–32
32. Wang W, Wang X, Zhou M, Yue J, Mao Q (2010) Novel NaY zeolite-supported nanoscale zero-valent iron as an efficient heterogeneous Fenton catalyst. J Catal Commun 11:937–941
33. Wang P, Cao M, Qian J, Wang Ch, Ao Y, Hou J (2014) Kinetics and thermodynamics of adsorption of methylene blue by a magnetic graphene-carbon nanotube composite. J Appl Surf Sci 290:116–124
34. Wu X, Huib KN, Lee SK, Huia KS, Hwang DH, Chen R, Zhoud W, Son YG, Cho YR (2012) Adsorption of basic yellow 87 from aqueous solution onto two different mesoporous adsorbents. Chem Eng J 180:91–98